OPTOELECTRONICS LETTERS Vol.12 No.1, 1 January 2016

Preparation and characterization of $In_{0.82}Ga_{0.18}As$ PIN photodetectors*

LIU Xia (刘霞)[1,2], **CAO Lian-zhen** (曹连振)[1,2]**, **LU Huai-xin** (逯怀新)[1], **LI Ying-de** (李英德)[1], **SONG Hang** (宋航)[2], **and JIANG Hong** (蒋红)[2]

1. *Shandong Provincial Key Laboratory of Multi-photon Entanglement and Manipulation, Department of Physics and Optoelectronic Engineering, Weifang University, Weifang 261061, China*
2. *Key Laboratory of Excited State Processes, Changchun Institute of Optics, Fine Mechanics and Physics, Chinese Academy of Sciences, Changchun 130033, China*

(Received 17 November 2015)

Using two-step growth method and buffer layer annealing treatment, the double heterojunction structures of $In_{0.82}Ga_{0.18}As$ epilayer capped with $InAs_{0.6}P_{0.4}$ layer were prepared on InP substrate by low pressure metal organic chemical vapor deposition (LP-MOCVD). Based on the high quality $In_{0.82}Ga_{0.18}As$ structures, the $In_{0.82}Ga_{0.18}As$ PIN photodetector with cut-off wavelength of 2.56 μm at room temperature was fabricated by planar semiconductor technology, and the device performance was investigated in detail. The typical dark current at the reverse bias V_R=10 mV and the resistance area product R_0A are 5.02 μA and 0.29 $\Omega\cdot cm^2$ at 296 K and 5.98 nA and 405.2 $\Omega\cdot cm^2$ at 116 K, respectively. The calculated peak detectivities of the $In_{0.82}Ga_{0.18}As$ photodetector are 1.21×10^{10} $cm\cdot Hz^{1/2}/W$ at 296 K and 4.39×10^{11} $cm\cdot Hz^{1/2}/W$ at 116 K respectively, where the quantum efficiency η=0.7 at peak wavelength is supposed. The results show that the detection performance of $In_{0.82}Ga_{0.18}As$ prepared by two-step growth method can be improved greatly.

Document code: A **Article ID:** 1673-1905(2016)01-0008-4

DOI 10.1007/s11801-016-5228-x

The $In_xGa_{1-x}As$/InP material systems have received increasing attention in many fields, such as photodiodes[1], infrared emitting and detecting devices[2] and high electron drift velocity devices[3], due to the wide band-gap energy range from 0.35 eV to 1.43 eV. Among the most important devices, the $In_{0.53}Ga_{0.47}As$/InP detectors for near-infrared light with cut-off wavelength up to 1.7 μm have been widely used for commercial and military fields[4,5]. In recent years, the $In_xGa_{1-x}As$ (x>0.53) detectors for extended infrared wavelength are greatly needed in applications, such as earth observation[6] and space imaging and spectroscopy[7]. As we known, $In_xGa_{1-x}As$ alloys with high In content grown on InP substrate can introduce a large lattice mismatch[8], which is believed to be the most limitation of $In_xGa_{1-x}As$ material quality, in this case an extraordinary buffer layer should be inserted to prevent the degradation of device performance. Many growth techniques of buffer layer[9,10] have been adopted to improve the quality of $In_xGa_{1-x}As$ alloys with high In content, in which two-step growth method is a convenient and effective way[11,12]. However, the material preparation and analysis of device performance of $In_{0.82}Ga_{0.18}As$ grown by two-step growth method have been rarely reported.

In this paper, the high quality $In_{0.82}Ga_{0.18}As$ materials were prepared by two-step growth method, and the thermal annealing treatments of buffer layer were used to improve the quality of epilayers. Based on the high quality epilayers, the planar $In_{0.82}Ga_{0.18}As$ PIN photodetectors were fabricated, and the device performances are characterized in detail.

All the samples were grown on semi-insulating (100) InP substrates in a horizontal reactor by low pressure metal organic chemical vapor deposition (LP-MOCVD) at the pressure of 10 kPa. The substrates were heated by inductively coupling radio frequency (RF) power, and temperatures were detected by a thermocouple. The growth was performed using trimethyl-indium (TMIn), trimethyl-gallium (TMGa) and arsine (AsH_3) diluted to 10% in H_2 as precursors.

The growth procedure and the parameters of $In_{0.82}Ga_{0.18}As$ epilayers were similar to those described in Refs.[11] and [13]. The schematic diagram of material structure of $In_{0.82}Ga_{0.18}As$ photodetector is shown in

---

* This work has been supported by the National Natural Science Foundation of China (Nos.11174224 and 11404246), the Natural Science Foundation of Shandong Province (Nos.BS2015DX015 and ZR2013FM001), the Science and Technology Development Program of Shandong Province (No.2013YD01016), and the Higher School Science and Technology Program of Shandong Province (Nos.J13LJ54 and J15LJ54).

** E-mail: lianzhencao@wfu.edu.cn

Fig.1. In the growth of $In_{0.82}Ga_{0.18}As$ material, the thermal-cleaning treating of InP substrate was carried in PH_3 gas at 630 °C for 10 min to remove the absorption of surface oxygen. Next, the substrate temperature was decreased to 450 °C to grow a thin $In_{0.82}Ga_{0.18}As$ buffer about 100 nm in thickness. Then, the buffer layer was thermal annealed at 530 °C in-situ for 5 min in AsH_3 gas atmosphere. After that, the $In_{0.82}Ga_{0.18}As$ absorption layer was grown on the annealed buffer layer at 530 °C with the thickness of about 2.9 μm[14]. Finally, $InAs_{0.6}P_{0.4}$ layer with thickness of about 0.9 μm was capped to reduce the surface recombination states and to increase the quantum efficiency of $In_{0.82}Ga_{0.18}As$ absorption layer.

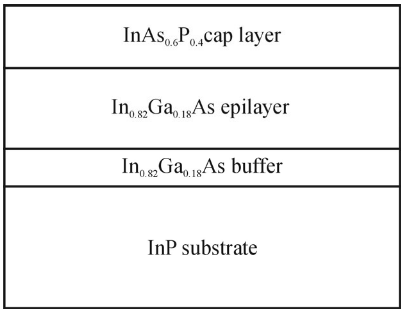

Fig.1 The schematic diagram of $In_{0.82}Ga_{0.18}As$ material structures capped with $InAs_{0.6}P_{0.4}$ layer with thickness of about 0.9 μm

After the growth, the $In_{0.82}Ga_{0.18}$ wafers were processed into planar-type detectors as follows. The wafers were firstly degreased in organic solvents, and passivated using SiO_2 compounds. Then the wafers were etched by standard lithography process to form the diffusion area and doped by Zn diffusion technique to form the P-N junction. And then the ohmic contact electrode was formed by evaporation, of which P and N contacts are Au/Zn/Au and Au, respectively. Finally, after the alloy step, the wafer was cut into chips for further measurements. The schematic diagram of cross section structure of the detector is shown in Fig.2.

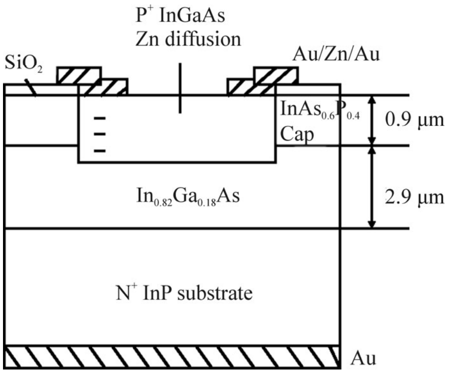

Fig.2 The schematic diagram of cross section of InGaAs photodetector

The structural characteristics of $In_{0.82}Ga_{0.18}As$ epilayers were measured by double-crystal X-ray diffraction (DCXRD, Bruker D8). The surface and cross section morphology of photodetectors were characterized by scanning electron microscopy (SEM, Hitachi S-4800). The current-voltage (*I-V*) characteristics were measured using a HP4156A precise semiconductor analyzer, which was installed in a close cycled helium cryostat to control the temperature. The response spectra of the detectors were measured by using a Nicolet 760 Fourier transform infrared (FTIR) spectrometer at room temperature.

The DCXRD spectrum of $InAs_{0.6}P_{0.4}/In_{0.82}Ga_{0.18}As/InP$ structure is shown in Fig.3. Only two peaks can be seen in the spectrum. One is InP substrate diffraction peak, and the other is $In_{0.82}Ga_{0.18}As$ diffraction peak, of which the In composition is calculated from the XRD pattern. It is implied that the diffraction peak of $InAs_{0.6}P_{0.4}$ cap layer completely coincides with $In_{0.82}Ga_{0.18}As$ peak because of the lattice match between them. In addition, the quality of $In_{0.82}Ga_{0.18}As$ absorption layer has been improved greatly by two-step growth method and buffer layer annealing treatment as reported in Refs.[11] and [13], according to the sharp diffraction peak of $In_{0.82}Ga_{0.18}As$.

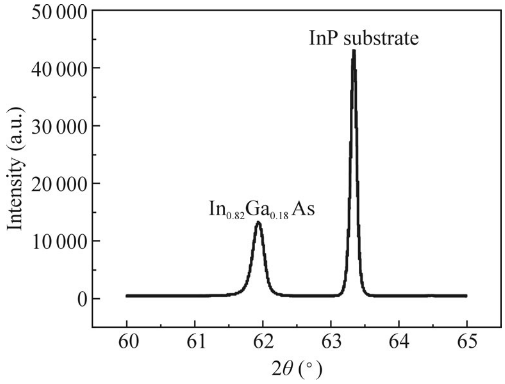

Fig.3 The DCXRD spectrum of $InAs_{0.6}P_{0.4}/In_{0.82}Ga_{0.18}As/InP$ structure

Fig.4 shows the surface and cross section morphology images of $InAs_{0.6}P_{0.4}/In_{0.82}Ga_{0.18}As/InP$ structure. From Fig.4(a), it can be seen that the surface of $In_{0.82}Ga_{0.18}As$ structure is smooth and nearly no pit exits. This indicates that the surface morphology of $In_{0.82}Ga_{0.18}As$ epilayers is improved obviously after the introduction of low temperature buffer layer, which is consistent with the results of XRD. Fig.4(b) displays the cross section photograph of InGaAs structure. It is seen that the InGaAs structure has a clear interface. All the results of XRD and SEM indicate that the InGaAs structure can meet the requirements of photodetectors.

Dark current is an important parameter to characterize the device performance of photodetectors. The analysis of InGaAs photodetector dark current is performed by measuring the reverse voltage of the *I-V* characteristic curve. The typical *I-V* characteristic curves of InGaAs photodetector are measured at the temperature from 116 K to 296 K with the step of 40 K and over seven orders of magnitude in current range, which are shown in Fig.5. It can be seen that at the reverse bias V_R=10 mV, the dark current decreases three orders of magnitude from 5.02 μA at 296 K to 5.98 nA at 116 K. To see the temperature effect on dark current curve more clearly, the curves of dark current versus reciprocal temperature at different reverse bias voltages are shown in Fig.6. It is seen that the whole area can be divided into three parts. When the temperature is higher than 230 K (area marked 1), the curve of current versus reciprocal temperature of detector is approximately linear, which can be fitted by formula of diffusion current. This indicates that the diffusion current is dominant in this temperature range[15]. When the temperature is lower than 150 K (area marked 3), the dark current drops further but with a lower slope, which may attribute to the tunneling current[16]. This means that the trap assisted tunneling current begins to play an important role in this temperature range. In the middle temperature range (area marked 2), both of them may determine the characteristic curve.

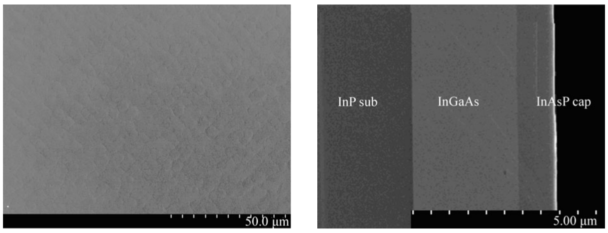

(a) Surface morphology (b) Cross section morphology

Fig.4 The morphology images of $In_{0.82}Ga_{0.18}As$ structure capped with $InAs_{0.6}P_{0.4}$ layer

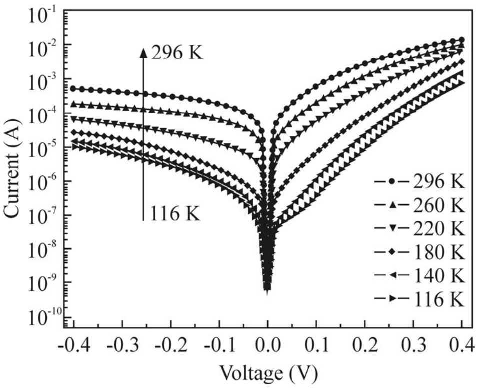

Fig.5 Measured typical *I-V* characteristics of the detectors in the temperature range from 116 K to 296 K in step of 40 K

The response spectrum of the $In_{0.82}Ga_{0.18}As$ photodetector was measured by using a Nicolet 760 FTIR spectrometer at room temperature and zero bias. Fig.7 shows the response spectrum of detector measured at room temperature. It can be seen that the response peak is about 2.0 μm with 50% cut-off wavelength of 2.56 μm, and the short wave cut-off wavelength is around 0.8 μm, which is determined by the energy band-gap of $InAs_{0.6}P_{0.4}$ cap layer. Using the measured response spectrum, it can be extrapolated that the quantum efficiency of the 2.56 μm detectors is great than 0.6 at the peak wavelength[8]. In addition, the fluctuations around 1.9 μm can be clearly seen in the response spectra, which may correspond to the water vapor absorption band in the air[2].

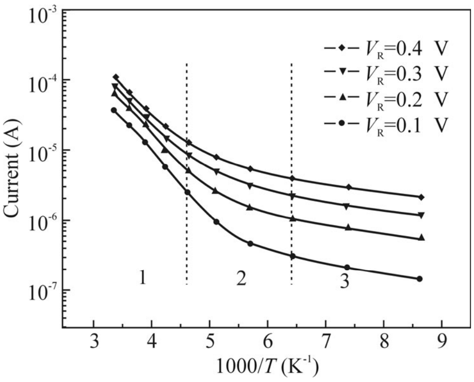

Fig.6 The plot of the dark current versus reciprocal temperature of the photodetector at various reverse bias voltages

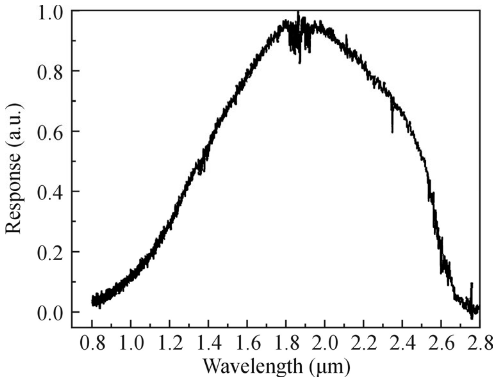

Fig.7 The response spectrum of the $In_{0.82}Ga_{0.18}As$ photodiodes measured at room temperature *T*=300 K

The detectivity D^* is the main parameter to characterize the performance of photodetectors. As we known, the key factors to improve the detectivity lie in increasing the zero-bias resistance area product (R_0A) and the quantum efficiency[17]. The resistances of the detectors at zero bias R_0 are also measured. The typical resistance area product R_0A versus reciprocal temperature of detectors is plotted in Fig.8. The R_0A of $In_{0.82}Ga_{0.18}As$ detector is about 0.29 Ω·cm^2 at 296 K. When the detector is cooled down to 116 K, R_0A increases exponentially to 405.2 Ω·cm^2. The calculated peak detectivity of the $In_{0.82}Ga_{0.18}As$ detector is 1.21×10^{10} cm·Hz$^{1/2}$/W at 296 K and 4.39×10^{11} cm·Hz$^{1/2}$/W at 116 K, respectively, and in the calculation the quantum efficiency η=0.7 at peak wavelength is supposed. Considering the detectivity of the $In_{0.82}Ga_{0.18}As$ detector is related to quantum efficiency, much work still should be done to increase the quantum efficiency for the optimization of device performance.

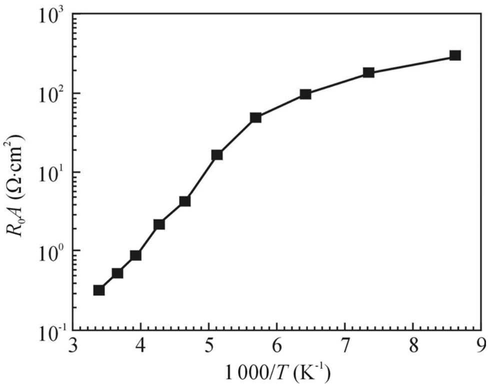

Fig.8 The resistance area product R_0A of the detectors measured at different temperatures

In conclusion, the $In_{0.82}Ga_{0.18}As$ PIN photodetectors with cut-off wavelength of about 2.56 μm at room temperature were grown by two-step growth method using LP-MOCVD. The structural characteristics and device performance are investigated in detail. According to the results of XRD and SEM, the quality of the structures is high which can meet the requirements of device fabrication. The typical dark current with reverse bias at V_R=10 mV and the resistance area product R_0A are 5.02 μA and 0.29 Ω·cm^2 at 296 K and 5.98 nA and 405.2 Ω·cm^2 at 116 K, respectively. Considering the quantum efficiency η=0.7 at peak wavelength, the calculated peak detectivity of the $In_{0.82}Ga_{0.18}As$ photodetector is 1.21×10^{10} cmHz$^{1/2}$/W at 296 K and 4.39×10^{11} cm·Hz$^{1/2}$/W at 116 K, respectively. The results indicate that the detection performance of $In_{0.82}Ga_{0.18}As$ photodetector grown by two-step growth method can be improved greatly.

References

[1] P. Kleinow, F. Rutz, R. Aidam, W. Bronner, H. Heussen and M. Walther, Infrared Physics & Technology **71**, 298 (2015).

[2] C. Li, Y. G. Zhang, K. Wang, Y. Gu, H. Li and Y. Y. Li, Infrared Physics & Technology **53**, 173 (2010).

[3] M. Liu, Y. M. Zhang, H. L. Lu, Y. M. Zhang, J. C. Zhang and X. T. Ren, Solid-State Electronics **109**, 52 (2015).

[4] J. Ajayan and D. Nirmal, Superlattices and Microstructures **86**, 1 **(**2015)

[5] Y. Arslan, F. Oguz and C. Besikci, Infrared Physics & Technology **70**, 134 (2015).

[6] H. J. Tang, X. L. Wu, K. F. Zhang, L. P. Ye, N. L. Wang, X. Li and H. M. Gong, Proceedings of SPIE **6835**, 683516-1 (2007).

[7] C. Li, Y. Zhang, Y. Gu, K. Wang, X. Fang, X. Li and H. Li, Infrared Physics & Technology **58**, 69 (2013).

[8] Y. G. Zhang , Y. Gu, C. Zhu, G. Q. Hao, A. Z. Li and T. D. Liu, Infrared Physics & Technology **47**, 257 (2006).

[9] X. Y. Chen, Y. Gu, Y. G. Zhang, S. P. Xi, Z. X. Guo, L. Zhou, A. Z. Li and Hsby. Li, Journal of Crystal Growth **425**, 346 (2015).

[10] R. Kumar, A. Bag, P. Mukhopadhyay, S. Das and D. Biswas, Applied Surface Science **357**, 922 (2015).

[11] X. Liu, H. Song, G. Q. Miao, H. Jiang, D. B. Li , X. J. Sun and Y. R. Chen, Applied Surface Science **257**, 1996 (2011) .

[12] X. Liu, L. Z. Cao, H. Song and H. Jiang, Optoelectronics Letters **10**, 269 (2014).

[13] X. Liu, H. Song, G. Q. Miao, H. Jiang, L. Z. Cao, D. B. Li, X. J. Sun, Y. R. Chen and Z. M. Li, Journal of Alloys and Compounds **509**, 6751 (2011) .

[14] Y. Gao, X. Gong, J. Li, G. Wu, Y. Feng, T. Makino and H. Kan, Journal of Optoelectronics·Laser **26**, 825 (2015). (in Chinese)

[15] Y. Zhao and S. He, Microelectronic Engineering **98**, 19 (2012).

[16] Y. Zhang, Y. Gu, Z. B. Tian, A. Z. Li, X. R. Zhu and Y. L. Zheng, Infrared Physics & Technology **51**, 316 (2008) .

[17] W. W. Chen, Y. Zhao, C. L. Yang, W. Qian, T. Q. Yang and J. Y. Yang, Journal of Optoelectronics·Laser **25**, 8 (2014). (in Chinese)